

Original Research

## PERMANENT MAGNET SYNCHRONOUS MOTOR TORQUE RIPPLE REDUCTION USING PREDICTIVE TORQUE CONTROL

Saif T. Bahar\*, Riyadh G. Omar

*Electrical Engineering Department, College of Engineering, Mustansiriyah University, Baghdad Iraq*

Received 26/6/2022

Accepted in revised form 23/9/2022

Published 1/5/2023

**Abstract:** The control a permanent magnet synchronous motors is the subject of this study and the torque ripple reduction in these motors is the main goal of this work. Torque and flux are controlled using a predictive model and vector control. Because it is commonly employed in regulating electric motors. Space vector control and predictive torque control are two permanent magnet synchronous motor control approaches used in this study. Predictive control was determined to be more effective in terms of response and action after a Mat lab simulation of the two approaches. Predictive torque control covers all potential switching states that decrease actual torque and flux ripples as well as total harmonic distortion. The benefits of predictive torque control include simple principles, an easy-to-use console, and the ability to implement limits quickly. However, there are some drawbacks to this technique, including the requirement for bigger accounts and faster machines. The fundamental principles of the control techniques discussed are provided. A permanent magnet synchronous motor powered by a two-level power converter is then used to simulate the control approaches. Their performance in comparison is based on the obtained results. An analytical model of the predictive torque control is presented utilizing SIMULINK to explain the operation.

**Keywords:** *Current ripple; torque ripple; predictive torque control*

### 1. Introduction

Permanent magnet synchronous motor (PMSM) drives are frequently utilized in great-performance applications such as robots,

aviation devices, and cars powered by electricity [1]. This fact arises because of their great power density, better torque per inertia, and good competence [2], [3]. For decades, Vector Control VC methods have been utilized to operate this type of motor well and keep its speed under control [4]. Model-predictive DTC (MPDTC) has been presented as a solution to several DTC issues. The essential idea behind MPC is to make certain predictions about potential future machine states using a discrete description of the system. The ideal voltage vector for a converter is chosen based on the prediction of machine states using an objective function that is minimized. Torque, flux, or switching frequency are typically the key optimization objectives for cost functions [5]–[6]. The torque and flux of the machine are controlled by a hysteresis-based switching table in the DTC drive. Moreover, the PMSM has excellent dynamic performance; steady-state ripples are still substantial. A suitable vector conversion is used in the VC technique to regulate decoupled torque and flux. Ripples in the stable equilibrium are reduced compared to DTC drives, and yet dynamic behavior is reduced. Model-predictive control (MPC) has

\*Corresponding Author: [ema2009@uomustansiriyah.edu.iq](mailto:ema2009@uomustansiriyah.edu.iq)

gained a lot of respect and interest in the power electronics and industrial drive communities in recent years. This MPC control approach, which was designed for process control applications and initially introduced in 1970, is widely used in industrial settings with a variety of applications. [7]. The controller's decision is either based on anticipated state variables and the accurate choice of control parameters, whether offline or live, or on the system's past state. Model-predictive control approaches are predicated on this basic notion. There is a considerable potential in the techniques of predictive current control (PCC) and predictive torque control [8]. The FCS-PTC technique offers many benefits in addition to reducing torque ripples, including the ability to easily accommodate limitations, uncomplicated construction, a simple algorithm, and quick dynamic reactions. The (MPDTC) approach works on the principle of calculating the appropriate control signals ahead of time [9]. Pulse width modulation is not required in the MPTC approach. As opposed to the DTC technique, the PTC technique has two disadvantages: first, it is speed-dependent, and second it takes time and effort to calculate. Following the application of the optimum objective function, The PTC method requires easily solved with a quicker and more efficient micro processing unit [8].

The frame of the paper is arranged as consequently: Section 2 explains the dynamic model of the PMSM, Section 3 explains the Three-Phase Converter Model, Section 4 explains Predictive Current, Section 5 explains Predictive Torque, Section 6 explains Cost Function, Section (7 explains Predictive Torque Control (PTC), Section 8 explains the Traditional Vector Control Scheme, and Section 9 explains Results.

## 2. Dynamic Model of the PMSM

The two-phase equivalent circuit approach is ideal for analyzing multiphase machinery. Inside a rotational d-q frame of reference, a mathematical formulation of PMSM may be constructed.

$$v_s = R_s * i_s + \frac{d\psi_s}{dt} \quad (1)$$

Where  $R_s$  is the stator resistance. The stator flux ( $\psi_s$ ) can be described as:

$$\psi_s = L_s * i_s + \psi_m * e^{j\theta_r} \quad (2)$$

Where  $L_s$  is the stator inductance,  $\psi_m$  is permanent magnet flux,  $\theta_r$  is the rotor angle. In addition, the voltage equations are obtained from the model are given by [10, 11].

$$v_s = R_s * i_s + L_s \frac{di_s}{dt} + j\psi_m * \omega_r * e^{j\theta_r} \quad (3)$$

$$V_{sq} = R_s * i_q + w_r * \Phi_d + Lq * \frac{d}{dt} i_q \quad (4)$$

$$V_{sd} = R_s * i_d - w_r * \Phi_q + Ld * \frac{d}{dt} i_d \quad (5)$$

Where  $w_r$  is rotor speed and  $Lq$  and  $Ld$  d-q stator inductance.  $i_q$  And  $i_d$  stator current. Flux linkages are given by,

$$\Phi_{sq} = Lq * i_q \quad (6)$$

$$\Phi_{sd} = Ld * i_d + \Phi_f \quad (7)$$

The actual torque is given by,

$$T_e = \frac{3}{2} \left( \frac{p}{2} \right) (\Phi_{sd} * i_q - \Phi_{sq} * i_d) \quad (8)$$

## 3. Three-Phase Converter Model

Figure 1 depicts the three-phase inverter circuit schematic used to convert the DC power to AC power. So, in order to avoid a DC supply short circuit, assume that any two switches in each inverter leg function in conjunction with one another.

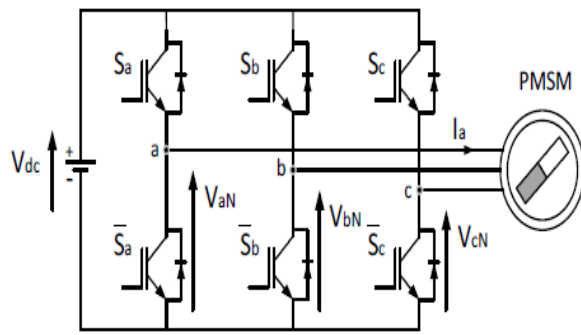


Figure 1. Circuit Diagram of the Three-Phase Inverter.

The implementation of switching combinations is as follows [9]:

$$S_a = \begin{bmatrix} 1 \text{ if } s1 \text{ ON and } s4 \text{ OFF} \\ 0 \text{ if } s1 \text{ OFF and } s4 \text{ ON} \end{bmatrix}$$

$$S_b = \begin{bmatrix} 1 \text{ if } s2 \text{ ON and } s5 \text{ OFF} \\ 0 \text{ if } s2 \text{ OFF and } s5 \text{ ON} \end{bmatrix}$$

$$S_c = \begin{bmatrix} 1 \text{ if } s3 \text{ ON and } s6 \text{ OFF} \\ 0 \text{ if } s3 \text{ OFF and } s6 \text{ ON} \end{bmatrix}$$

$$S = \frac{2}{3} (S_a - aS_b - a^2S_c) \tag{9}$$

Where  $a = e^{j\frac{2\pi}{3}} = \frac{-1}{2} + j\frac{\sqrt{3}}{2}$ .Deduced relationship between output voltage vector and change in the state of the switch may be deduced [10, 11]:

$$V_{out} = SV_{dc} = \frac{2V_{dc}}{3} (S_a - aS_b - a^2S_c) \tag{10}$$

Where,  $V_{dc}$  is the dc-link voltage and  $V_{out}$  is the output voltage at inverter terminals.

Eight alternative voltage vectors are produced by considering the various switching states of the inverter; this can be illustrated in Table 1. It is worth noting that ( $V_0 = V_7$ ) [7].

S <sub>a</sub>	S <sub>b</sub>	S <sub>c</sub>	V
0	0	0	$v_0 = 0$
1	0	0	$v_1 = \frac{2V_{dc}}{3}$
1	1	0	$v_2 = \frac{V_{dc} + j\sqrt{3}V_{dc}}{3}$
0	1	0	$v_3 = \frac{-V_{dc} + j\sqrt{3}V_{dc}}{3}$
0	1	1	$v_4 = \frac{-2V_{dc}}{3}$

0	0	1	$v_5 = \frac{-V_{dc}}{3} - j\frac{\sqrt{3}V_{dc}}{3}$
1	0	1	$v_6 = \frac{V_{dc}}{3} - j\frac{\sqrt{3}V_{dc}}{3}$
1	1	1	$v_7 = 0$

#### 4. Predictive Current

The algorithm can be used to discretize according the core idea of predictive control [12]. The sample period  $T_s$  is used, at the same time, the (k+1) time current is predictive (k).

$$i_{sd}(k+1) = \left(1 - \frac{R_s * T_s}{L_d}\right) i_{sd} + \left(\frac{w_r * L_q * T_s}{L_d}\right) i_{sq} + \left(\frac{T_s}{L_d}\right) V_{sd} \tag{11}$$

$$i_{sq}(k+1) = \left(1 - \frac{R_s * T_s}{L_q}\right) i_{sq} - \left(\frac{w_r * L_d * T_s}{L_q}\right) i_{sd} + \left(\frac{T_s}{L_d}\right) V_{sq} - \frac{w_r * \Phi_f * T_s}{L_q} \tag{12}$$

#### 5. Predictive Torque

Discretization is another use of the Euler method. The sampling time is  $T_s$ , and the (k+1) time current is predicted at time (k) using this data.

$$\Phi_{sq}(k+1) = L_q * i_{sq}(k+1) \tag{13}$$

$$\Phi_{sd}(k+1) = L_d * i_{sd}(k+1) + \Phi_f \tag{14}$$

$$\Phi_s(k+1) = \sqrt{(\Phi_{sd}(k+1))^2 + (\Phi_{sq}(k+1))^2} \tag{15}$$

$T_e(k+1)$  Is the predictive torque [13]:

$$T_e(k+1) = \frac{3}{2} \left(\frac{p}{2}\right) (\Phi_{sd}(k+1) * i_{sq}(k+1) - \Phi_{sq}(k+1) * i_{sd}(k+1)) \tag{16}$$

#### 6. Cost Function

Developing a non-negative function that measures the expected system state's distance from the intended values supplied by the reference and extra control goals is necessary. There are also the following correlations with two variables of varying magnitudes in these cost-function structures[14,15].Predictive torque and flux, which takes into account the associated cost function, [16,17]. Cost function

of PMSM drive controlled by traditional PTC is provided.

$$g = \left(\frac{T_{ref} - T_e(k+1)}{T_{ref}}\right)^2 + \lambda \cdot \left(\frac{\Phi_{ref} - \Phi_s(k+1)}{\Phi_{ref}}\right)^2 \quad (17)$$

Where  $T_{ref}$  and  $\Phi_{ref}$  are reference torque and reference flux value,  $T_e(k+1)$  and  $\Phi_s(k+1)$  are predictive torque and flux predictive value.  $\lambda$  is a weight factor.

### 7. Predictive Torque Control (PTC)

Figure 2 shows (PTC) created on FCS-MPC for 3-phase 2-L (PMSM) drives as described in [18, 19]. The stator flux and torque are the controllable variables, and they are managed by an external PI based speed control and an internal PTC[20]. During base speed operation, the stator flux reference is set to its nominal value, while the torque reference comes from an outside PI that changes with the speed error. The cost function is then assessed, and the VSI is switched to the switching state with the lowest cost (g).

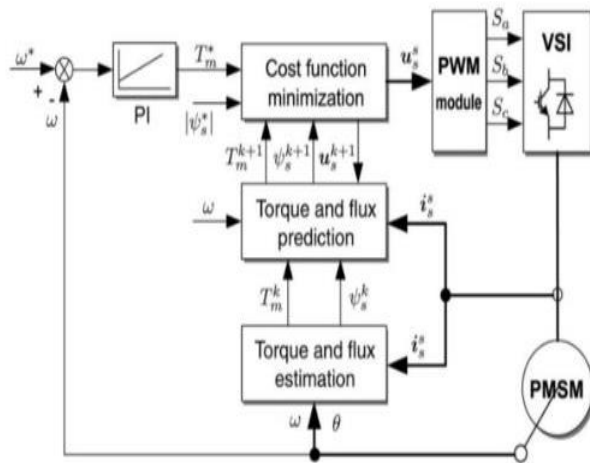


Figure 2. Block diagram of the (PTC) [21].

### 8. Traditional Vector Control Scheme

Vector of PMSM at concurrently is known as vector control. Using the Park and Clarke transform, the stator currents are transformed into space vector form with two orthogonally

elements  $i_{sd}$  and  $i_{sq}$ . One of the essential goals for VC is to separate the control of torque and flux. Torque is generated by  $i_{sq}$  and  $i_{sd}$  is generated by  $i_{sd}$ . The PI controller is used to regulate both currents independently. The flux component's reference current is set to zero, whereas the torque component's reference current is generated from speed controller. Figure 3 shows Vector Control Scheme.

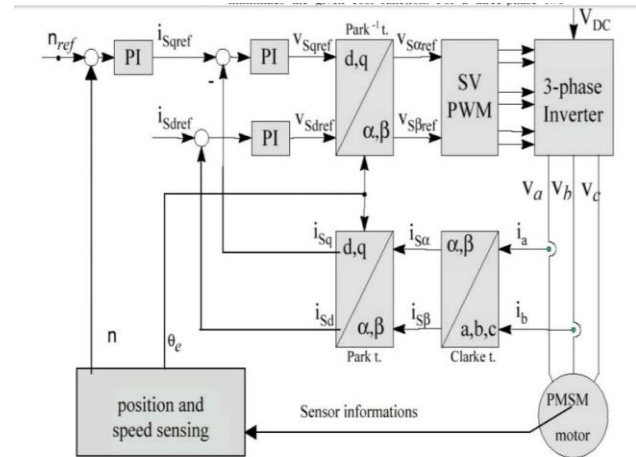


Figure 3. Block diagram of Vector Control Scheme [22].

### 9. Results

The simulation is carried out via Matlab/Simulink 2021 package. The system parameters are: Rated power=2.7kW, Rated speed ( $\omega_m$ )=3000rpm, Dc- link voltage =300V,  $p = 3$ ,  $L_d = 9$  mH,  $L_q = 9$  mH,  $R_s = 1.3\Omega$ , load torque = 8.5 Nm, flux = 0.41 wb,  $F = 50$  Hz,  $J = 0.0008$  kg.m<sup>2</sup>,  $T_s = 1$  μs. Figure 4 describe the algorithm flow chart. It is necessary to avoid two situations in order to use the suggested MPC algorithm. The method determines the best voltage vector for a particular cost function, which is subsequently employed in predictive direct torque control. As shown in figure 2. MPC has far fewer fluxes and torque ripples than Vector Control. Figure 9 shows that when utilizing MPC, the inverter current THD is lower than the THD in Vector Control.

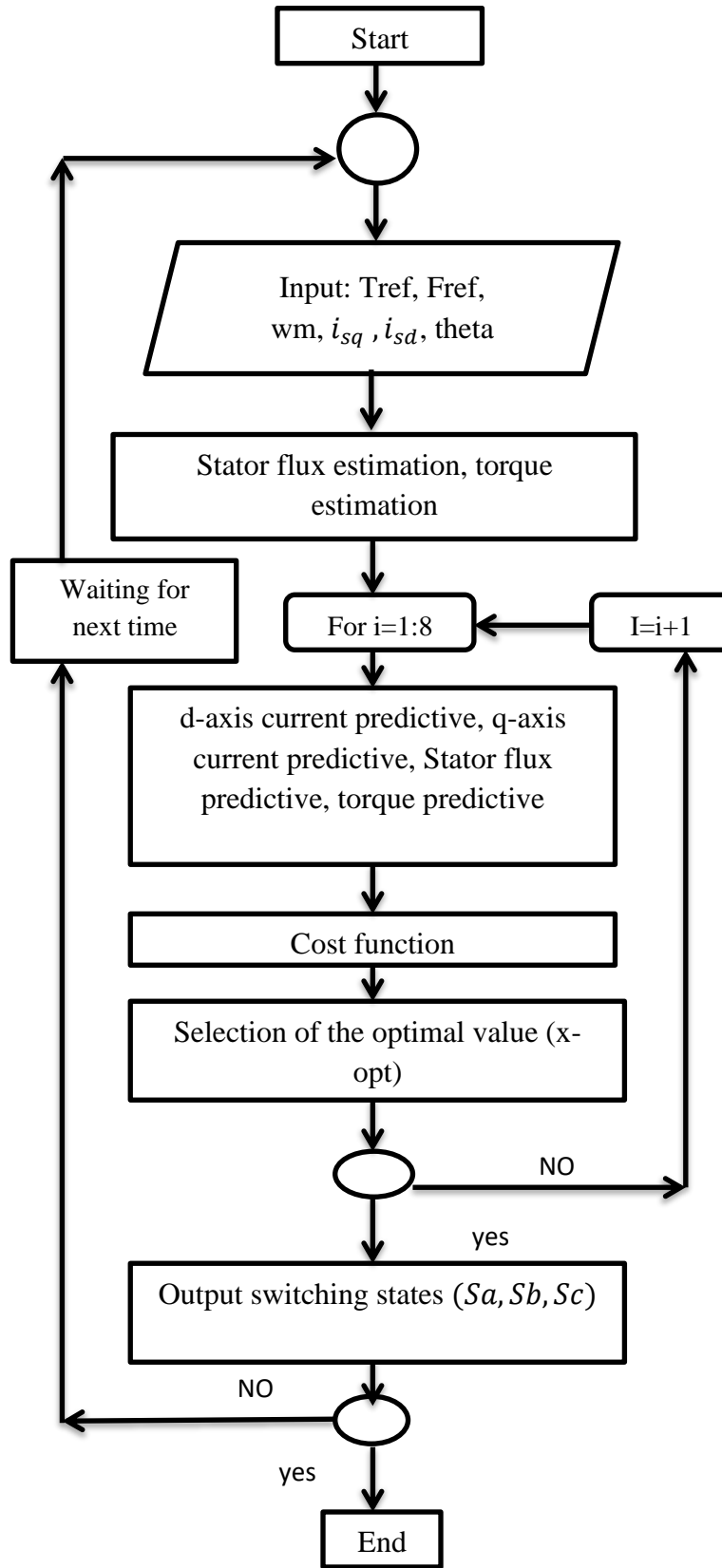


Figure 4. Flow chart of the MPTC

Figure 5 shows Simulink/MATLAB for Vector Control Scheme.

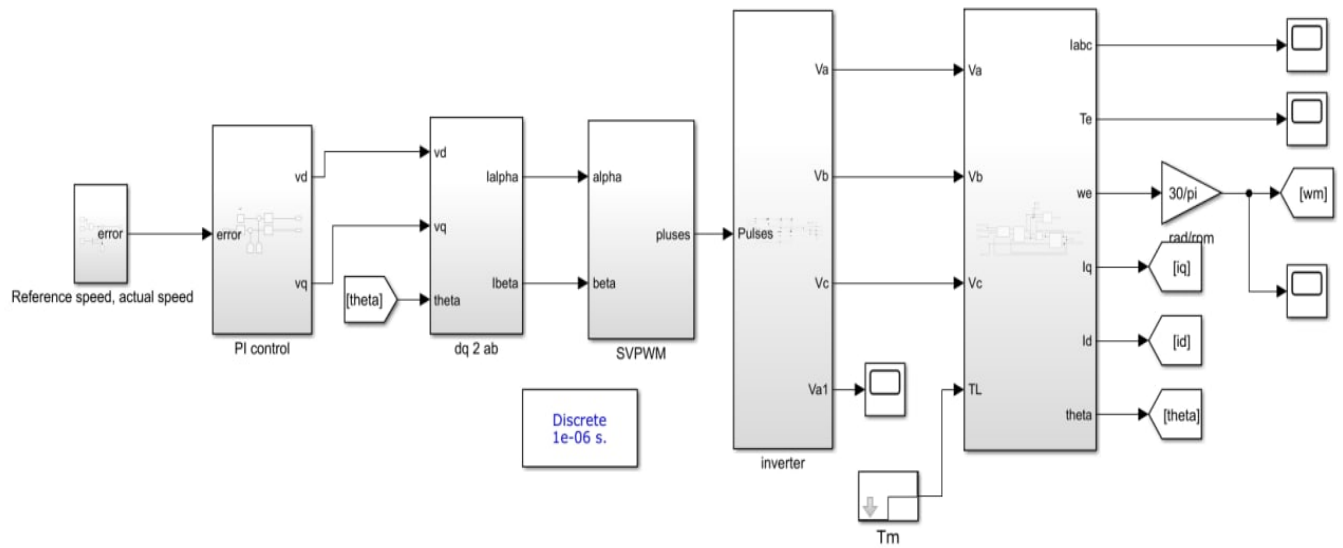


Figure 5. Simulink/MATLAB Vector Control Scheme

Figure 6 shows Simulink/MATLAB for Model Predictive Torque Control (PTC).

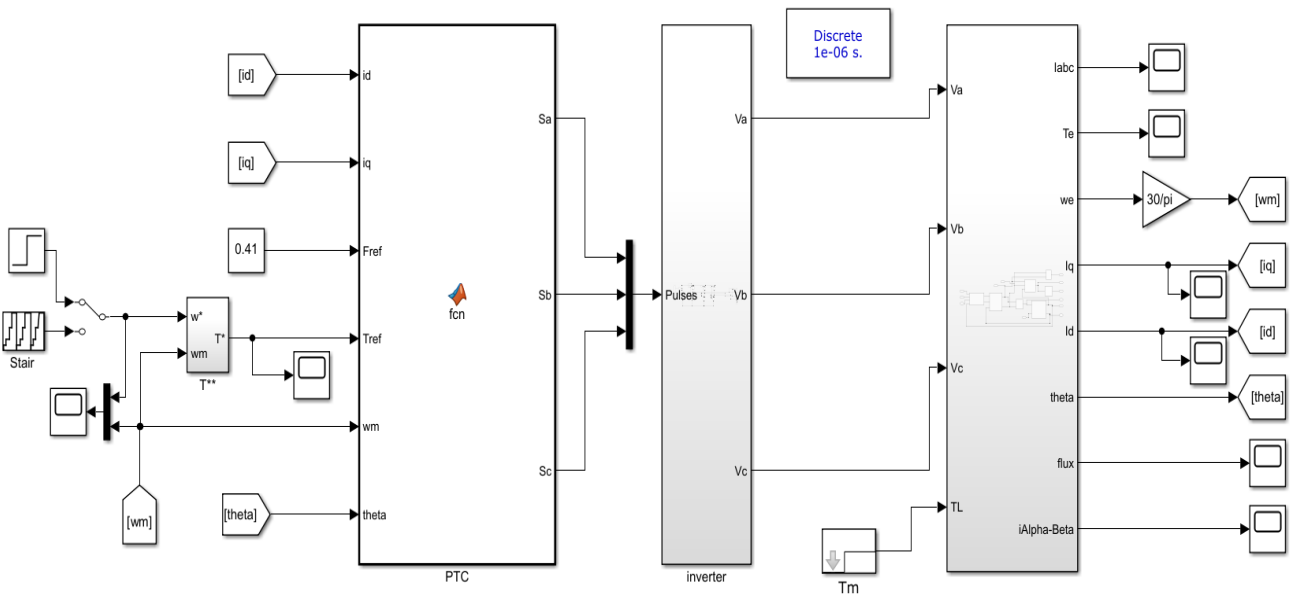


Figure 6. Simulink/MATLAB Model Predictive Torque Control (PTC).

### 9.1. Steady-State Performance

Forms of rotor speed, electromagnetic torque, and stator current at steady state are displayed in figures below for two different control methods. The load torque is set at 8 Nm, and the reference speed is 3000 rpm.

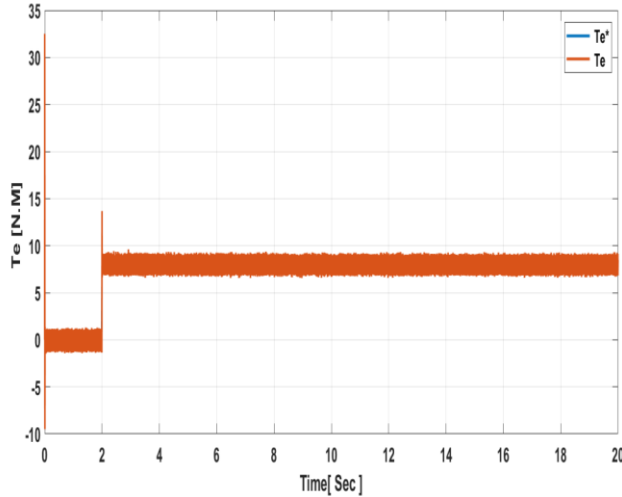


Figure 7. Actual torque and reference torque for Vector Control Scheme.

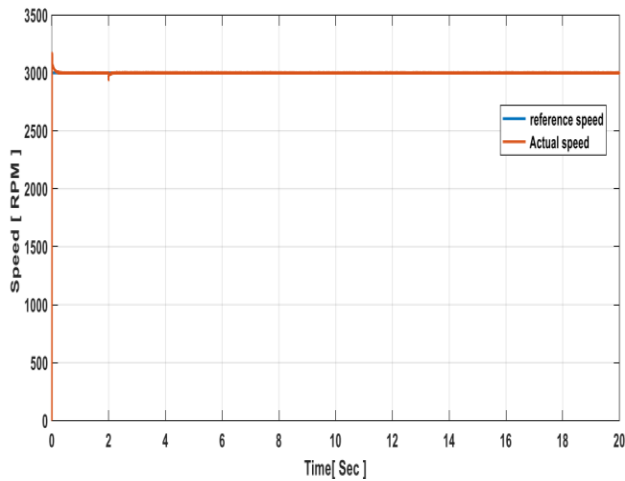


Figure 8. Actual speed and reference speed for Vector Control Scheme

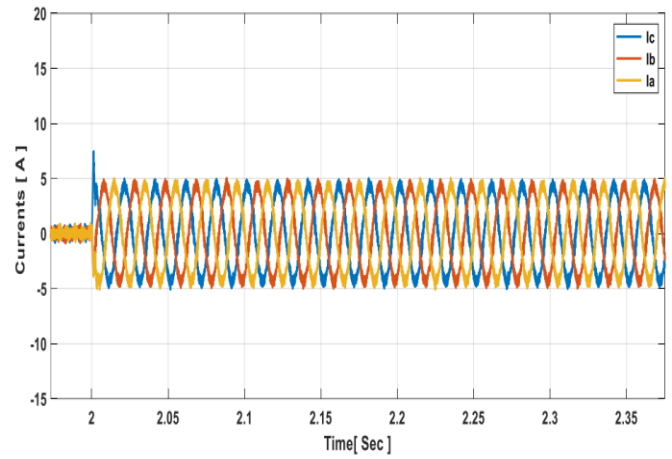


Figure 9. Measured three phases stator currents for Vector Control Scheme

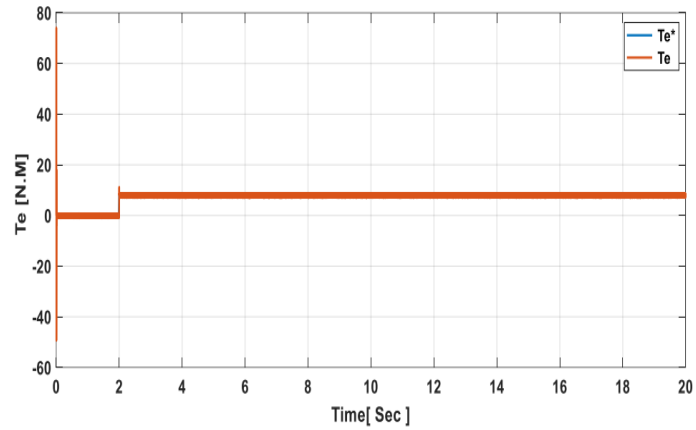


Figure 10. Actual torque and reference torque for Model Predictive Torque Control .

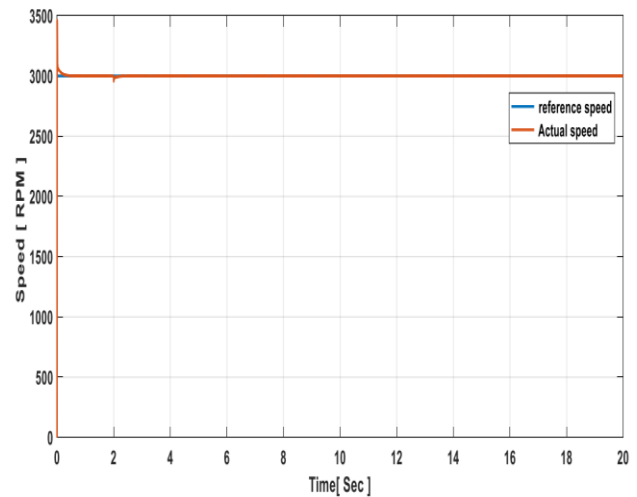
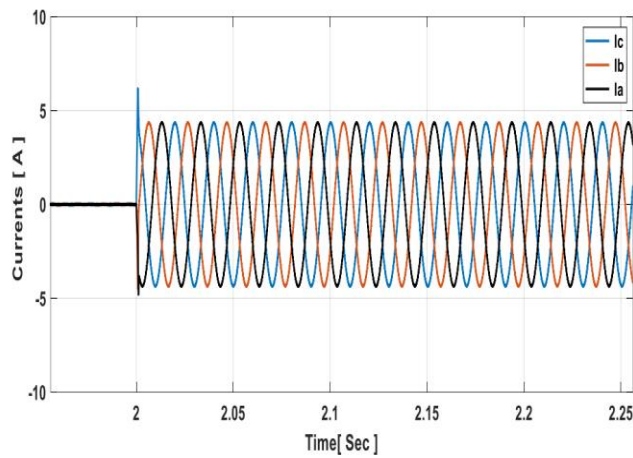
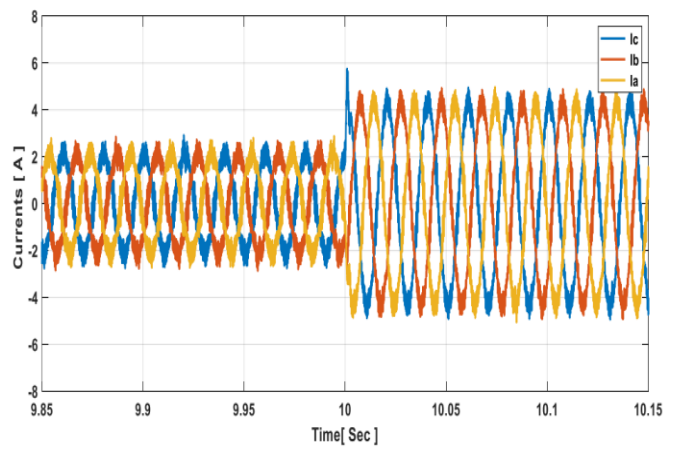


Figure 11. Actual speed and reference speed for Model Predictive Torque Control.



Figures 12. measured three phases stator currents for Model Predictive Torque Control



Figures 14. measured three phases stator currents for Vector Control Scheme

### 9.2. Dynamic Response

Dynamic responses of two control systems are evaluated and displayed in figures below, in addition to the steady-state performance. After 10 seconds, the load torque increases from 4Nm to 8.5 Nm, while the rotor speed is changes (0, 400, 800, 1800 ,3000) rpm.

Figures 13 and 14 show the measured three phases stator currents for Model Predictive Torque Control (PTC) and Vector Control Scheme

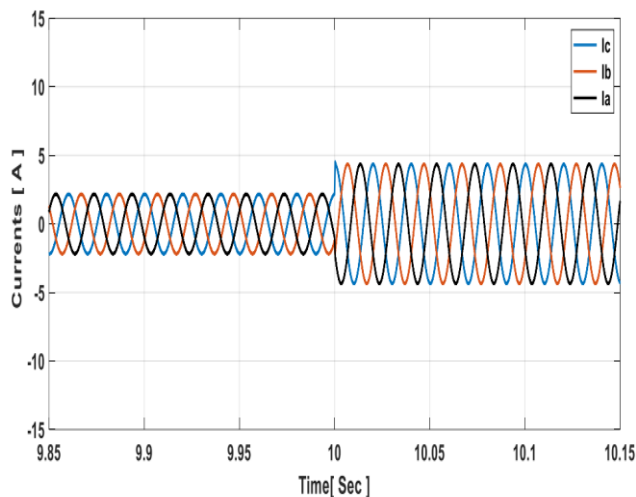


Figure 13. measured three phases stator currents for Model Predictive Torque Control

Figure 15 and 16 presents the harmonics contain, also the result in this figure shows the MPTC excellent THD in the stator current with PMSM drive.

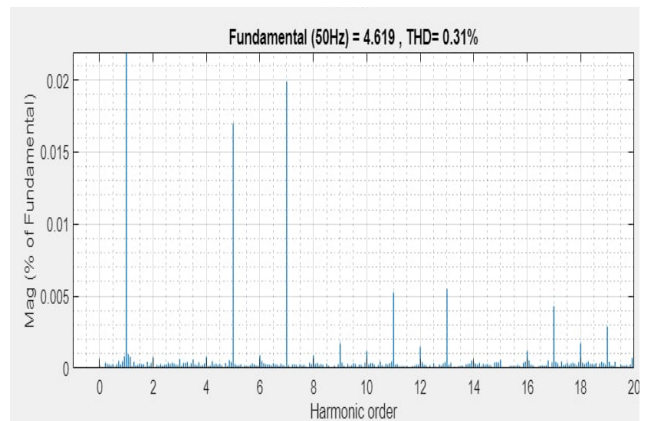
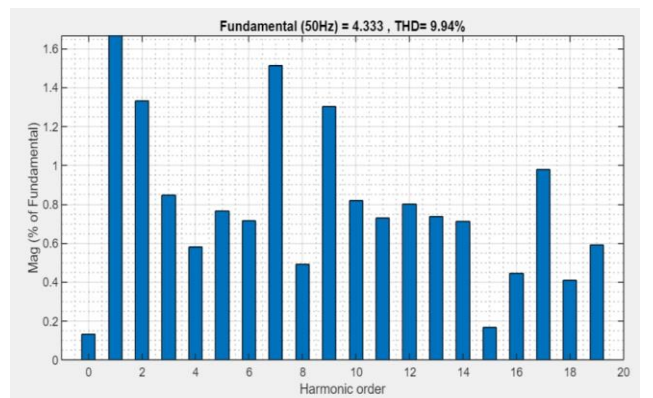
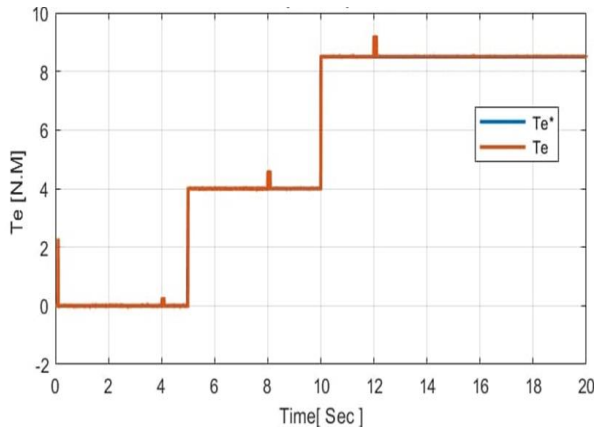


Figure 15. Total Harmonic Distortion for Model Predictive Torque Control.

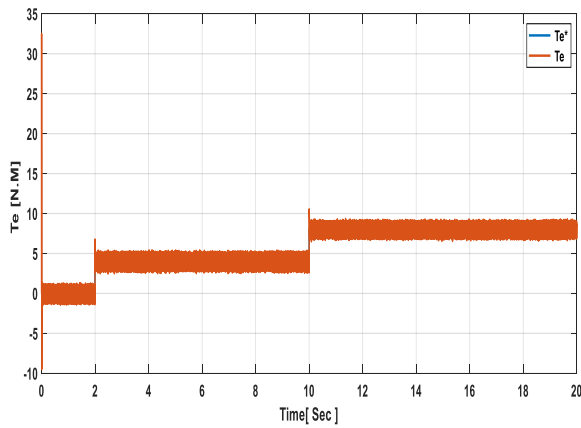


**Figure 16.** Total Harmonic Distortion for Vector Control Scheme.

Figure 17, 18 shows Actual torque, and reference torque generating from the PI controller. The load torque is change (0, 4, 8.5 Nm).

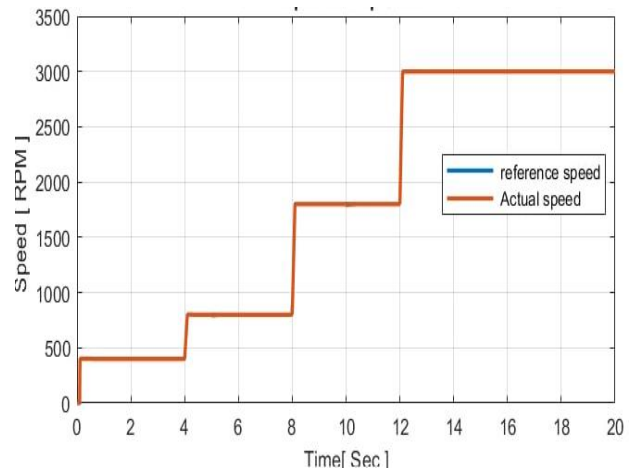


**Figure 17.** Actual torque and reference torque for Model Predictive Torque Control .



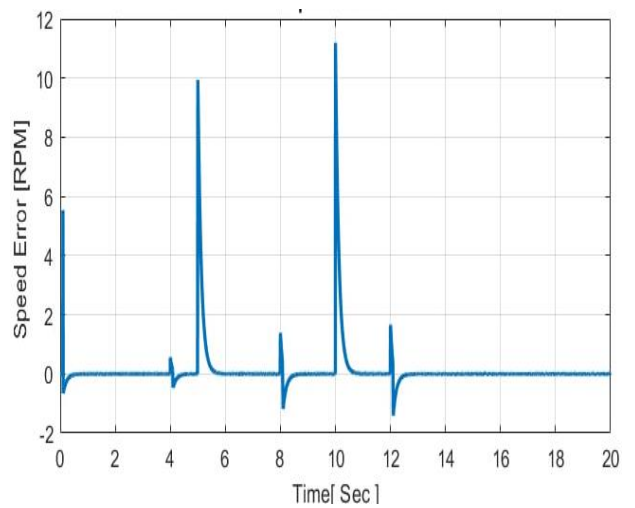
**Figure 18.** Actual torque and reference torque for Vector Control Scheme.

Figure 19 shows the reference speed, actual speed.



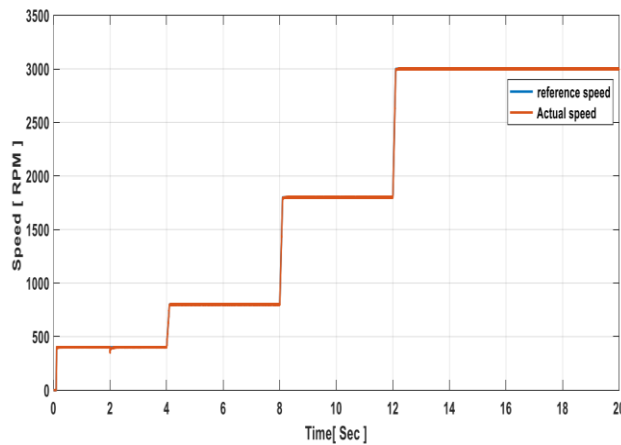
**Figure 19.** Actual speed and reference speed for Model Predictive Torque Control.

Figure 20 shows the errors among Actual speed and reference speed.



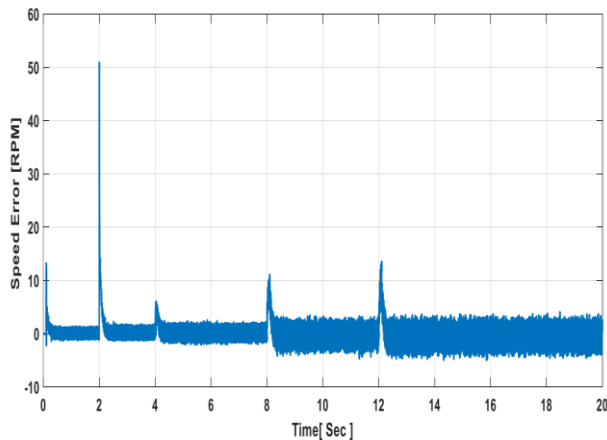
**Figure 20.** Error for Model Predictive Torque Control.

Figure 21 shows the reference speed, actual speed.



**Figure 21.** Actual speed and reference speed for Vector Control Scheme.

Figure 22 shows the errors among Actual speed and reference speed.



**Figure 22.** Error for Vector Control Scheme.

The results showed an error decrease in the speed and the motor torque disparity. Moreover, the THD is enhanced. And this strategy can be utilized in applications that required such values. The reliability and robustness of the control system are also demonstrated by the outcomes achieved and the necessary costs. Table (2) demonstrated the conclusion of a comparison between the results of PTC and Vector Control.

**Table 2** .comparison between of PTC and Vector Control

Results	PTC	Vector Control
Tracking speed	Less	Good
Torque ripple	Good	bad
THD (%)	0.31%	9.94%
Current ripple	Good	bad

## 10. Conclusions

The control of (PMSM) is the subject of this study and the torque ripple reduction in the (PMSM) is the main goal of this work. Torque and flux are controlled using a predictive model and Vector Control. Because it is commonly employed in regulating electric motors, MPC covers all potential switching states that decrease torque and flux ripples as well as THD. PTC provides fast dynamic response, according to a comparison of the two approaches. Future work will involve testing switched reluctance motors and using PTC method to servomotors with 2-level VSI and multilevel inverters.

The following points illustrate the contribution to the paper:

1. Torque ripple is less in PTC opposite method vector control.
2. Vector control THD is larger than the predictive control. Notice that the value of THD in vector control (9.94%) is much greater than that of THD in PTC (0.31%).
3. Because of this, predictive control is favored for PMSM control, which results in lower torque ripple and lower THD than conventional control.

## Acknowledgements

To the teachers of Mustansiriyah University, the writers would like to express their thanks for their aid and advice.

## Conflict of interest

The authors declare that there are no conflicts of interest regarding the publication of this manuscript.

## Abbreviations

$\Phi$	Flux
$\lambda$	weight factor
$\psi_m$	permanent magnet flux
$\theta_r$	rotor angle

## Author Contribution Statement

Authors Saif T. Bahar and Riyadh G. Omar: suggested the study problem. Two authors develop the results. The contribution to the paper is to reduce torque ripple, reduce distortions in current, and reduce Total Harmonic Distortion.

## References

1. T. Khawish Hassan and Z. Mahmood Abed, "V/f Speed Control of Five-Phase Permanent Magnet Synchronous Motor Fed By Indirect Matrix Converter With Carrier-Based PWM", *jeasd*, vol. 23, no. 2, pp. 141–165, Mar. 2019. <https://doi.org/10.31272/jeasd.23.2.12>
2. Asaei, B., & Rahrovi, B. (2010). Minimum-copper-loss control over full speed range of an IPMSM drive for hybrid electric vehicle application. In 2010 IEEE vehicle power and propulsion conference (pp. 1-6). IEEE. <https://doi.org/10.1109/vppc.2010.5728999>
3. Z. Zhou, C. Xia, Y. Yan, Z. Wang and T. Shi, (2017). "Torque Ripple Minimization of Predictive Torque Control for PMSM with Extended Control Set," in IEEE Trans. Ind. Electron., vol. 64, no. 9, pp. 6930-6939. <https://doi.org/10.1109/TIE.2017.2686320>
4. F. Niu, B. Wang, A. S. Babel, K. Li and E. G. Strangas, (2016). "Comparative Evaluation of Direct Torque Control Strategies for Permanent Magnet Synchronous Machines," in IEEE Trans. Power Electron., vol. 31, no. 2, pp. 1408-1424, <https://doi.org/10.1109/tpel.2015.2421321>
5. S. Ouni, M. R. Zolghadri, M. Khodabandeh, M. Shahbazi, J. Rodríguez, H. Oraee, et al., (2017). "Improvement of Post-Fault Performance of a Cascaded H-bridge Multilevel Inverter," IEEE Transactions on Industrial Electronics, vol. 64, pp. 2779-2788, <https://doi.org/10.1109/TIE.2016.2632058>
6. M. Khodabandeh, M. R. Zolghadri, and N. Noroozi, (2015). "A new t-type direct AC/AC converter," in the 6th Power Electronics, Drive Systems & Technologies Conference (PEDSTC2015), pp. 247-252. <https://doi.org/10.1109/PEDSTC.2015.7093282>.
7. Thomas Burtscher and Tobias Geyer, (2013). "Deadlock Avoidance in Model Predictive Direct Torque Control," IEEE Transactions on Industry Applications, Vol. 49, No. 5. <https://doi.org/10.1109/TIA.2013.2261445>
8. Fengxiang Wang, Member, IEEE, Shihua Li, Senior Member, IEEE, Xuezhu Mei, Wei Xie, Member, IEEE, José Rodríguez, Fellow, IEEE, and Ralph M. Kennel, Senior Member, IEEE, (2015). "Model-Based Predictive Direct Control Strategies for Electrical Drives: An

- Experimental Evaluation of PTC and PCC Methods,” IEEE Transactions on Industrial Informatics, Vol. 11, No. 3.  
<https://doi.org/10.1109/TII.2015.2423154>
9. James Scoltock, Tobias Geyer and Udaya K. Madawala, (2013). “A Comparison of Model Predictive Control Schemes for MV Induction Motor Drives,” IEEE Transactions on Industrial Informatics, Vol. 9, No. 2.  
<https://doi.org/10.1109/TII.2012.2223706>
  10. Wang, T., Liu, C., Lei, G., Guo, Y., & Zhu, J. (2017). Model predictive direct torque control of permanent magnet synchronous motors with extended set of voltage space vectors. IET Electric Power Applications, 11(8), 1376-1382.  
<https://doi.org/10.1049/iet-epa.2016.0870>
  11. Li, H., Li, M., Zheng, C., & Chen, B. (2019). Comparison between Modified MPC and DTC Control Method for Permanent Magnet Synchronous Motor. In E3S Web of Conferences (Vol. 115, p. 02004). EDP Sciences.  
<https://doi.org/10.1051/e3sconf/201911502004>
  12. Xie, W., Wang, X., Wang, F., Xu, W., Kennel, R. M., Gerling, D., & Lorenz, R. D. (2015). Finite-control-set model predictive torque control with a deadbeat solution for PMSM drives. IEEE Transactions on Industrial Electronics, 62(9), 5402-5410.  
<https://doi.org/10.1109/TIE.2015.2410767>.
  13. Liu, Q., & Hameyer, K. (2016). Torque ripple minimization for direct torque control of PMSM with modified FCSMPC. IEEE Transactions on Industry Applications, 52(6), 4855-4864.  
<https://doi.org/10.1109/TIA.2016.2599902>
  14. J. Rodriguez, and P. Cortes, (2012). "Predictive Control of Power Converters And Electrical Drives", first edition, a John Wiley & Sons, Ltd. Publication.  
<https://doi.org/10.1002/9781119941446>
  15. Kusuma, E., Eswar, K. M. R., & Kumar, T. V. (2020). An effective predictive torque control scheme for PMSM drive without involvement of weighting factors. IEEE Journal of Emerging and Selected Topics in Power Electronics, 9(3), 2685-2697.  
<https://doi.org/10.1109/JESTPE.2020.2989429>
  16. Omar, R. G., & Ali, A. K. (2020). Switching Losses Constraint in Model predictive Direct Current Control with 3Ø Voltage Source Inverter to Drive Induction Motor.  
<https://doi.org/10.31272/jeasd.conf.1.18>
  17. Omar, R. G. (2020). Coast function parameters optimization for DC battery source inverter feeding three-phase inductive load. International Journal of Power Electronics and Drive Systems, 11(4), 1799.  
<https://doi.org/10.11591/ijpeds.v11.i4.pp1799-1804>
  18. Ma, Z., Saeidi, S., & Kennel, R. (2014). FPGA implementation of model predictive control with constant switching frequency for PMSM drives. IEEE transactions on industrial informatics, 10(4), 2055-2063.  
<https://doi.org/10.1109/TII.2014.2344432>
  19. Thangarajan, K., & Soundarajan, A. (2020). Performance comparison of permanent magnet synchronous motor (PMSM) drive with delay compensated predictive controllers. Microprocessors and Microsystems, 75, 103081.  
<https://doi.org/10.1016/j.micpro.2020.103081>
  20. A. Ahmed obed and M. Abdul Hameed Salman, “REDUCTION OF RIPPLE FOR

- DIRECT TORQUE CONTROLLED THREE PHASE INDUCTION MOTOR BASED ON A PREDICTIVE CONTROL TECHNIQUE”, *jeasd*, vol. 22, no. 6, pp. 72–84, Nov. 2018.  
<https://doi.org/10.31272/jeasd.2018.6.7>
21. Ma, Z., Saeidi, S., & Kennel, R. (2014). FPGA implementation of model predictive control with constant switching frequency for PMSM drives. *IEEE transactions on industrial informatics*, 10(4), 2055-2063.  
<https://doi.org/10.1109/tii.2014.2344432>
22. Liu, Tingting, Guojin Chen, and Shigang Li. "Application of vector control technology for PMSM used in electric vehicles." *The Open Automation and Control Systems Journal* 6.1 (2014).  
<https://doi.org/10.2174/1874444301406011334>